

## Supplementary Information

### MoS<sub>2</sub> nano flakes with self-adaptive contacts for efficient thermoelectric energy harvesting

Qingqing Wu, Hatef Sadeghi\*, Colin J. Lambert\*

Quantum Technology Centre, Physics Department, Lancaster University, LA1 4YB Lancaster, UK.

\**h.sadeghi@lancaster.ac.uk*; *c.lambert@lancaster.ac.uk*

#### 1. Band structure of MoS<sub>2</sub>

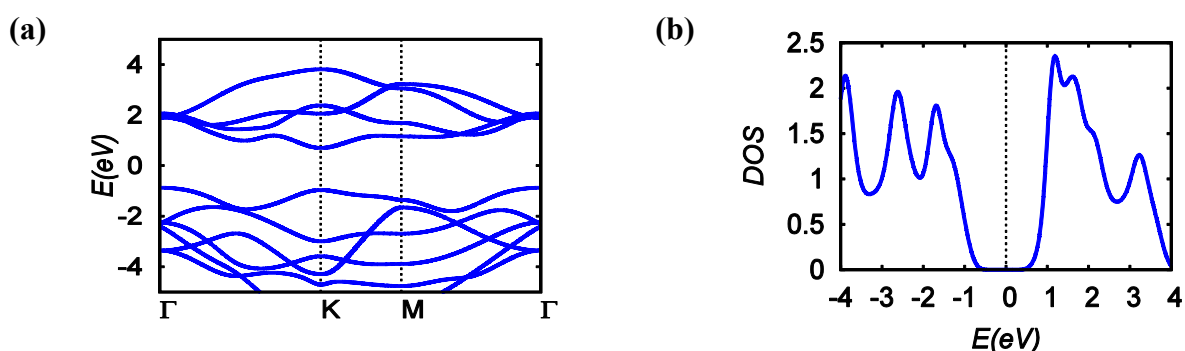


Fig. S1 The band structure and density of states of a two dimensional Mo<sub>2</sub>S monolayer.

#### 2. Transport properties of a metallic MoS nanowire

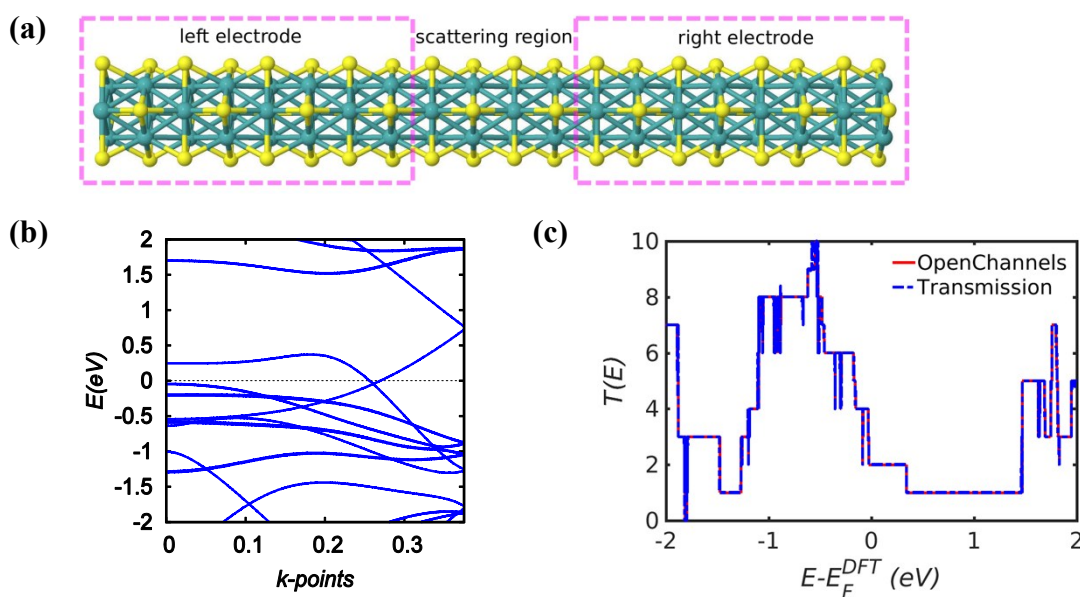


Fig. S2 (a) A schematic model of a MoS nanowire; (b), (c) the band structure of a pristine one dimensional wire and the electron transport properties of a sandwich junction.

### 3. Transport through two central regions with different lengths

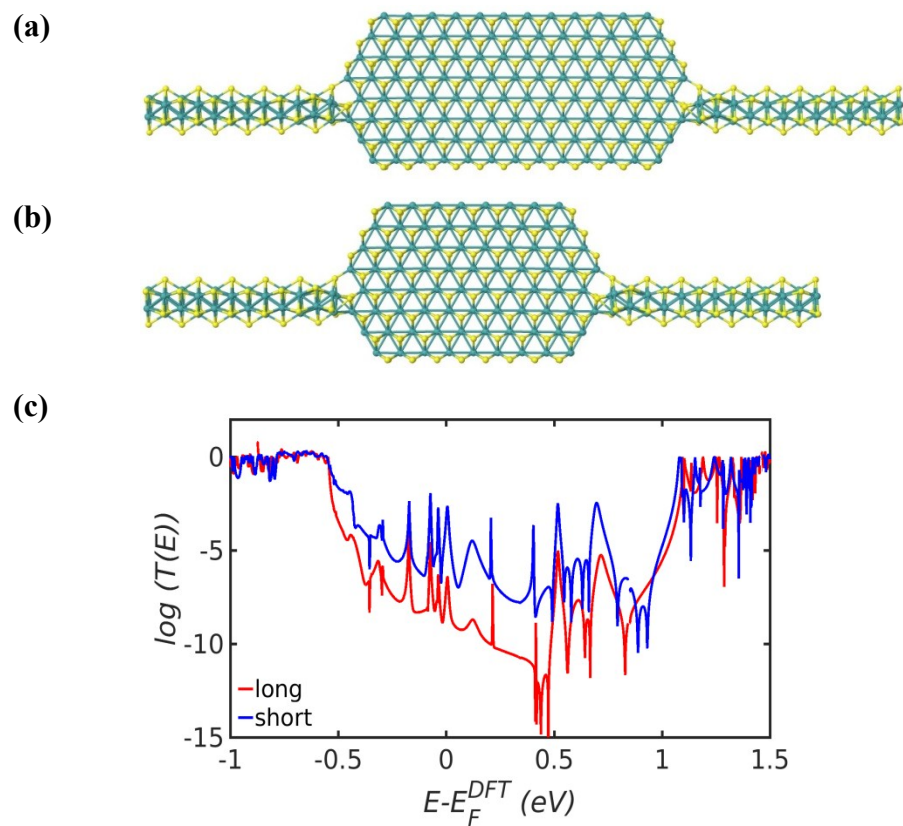
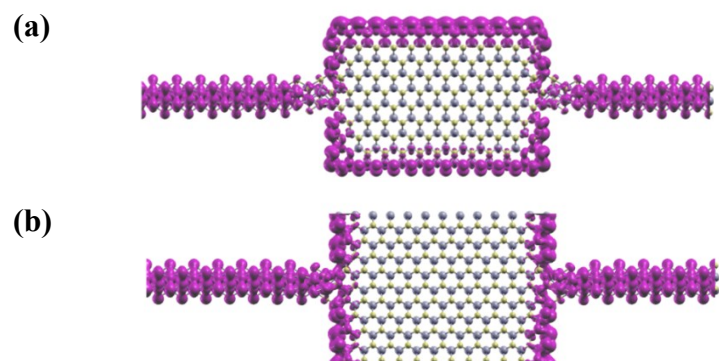


Fig. S3 (a) Schematic models 11, 22, 33 of nanoelectric devices with different length for  $\text{Mo}_2\text{S}$  scattering region; (b) the corresponding transmission spectra.

### 4. LDOS of junctions with rectangular edges



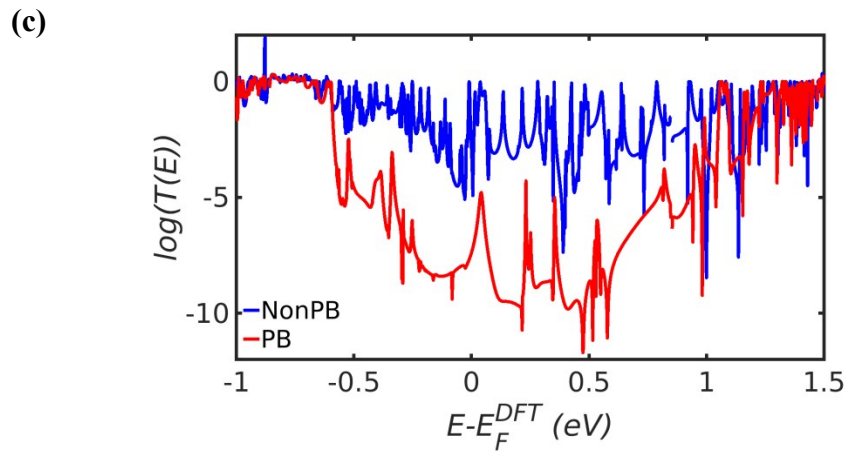


Fig. S4 (a), (b) The local density of states with and without periodic boundary conditions for the structure shown in Fig. S5(a) ; (c) the electron transmission spectra in these two cases.

### 5. The effect of symmetry of the junctions

To probe the effect of shifting the axis of the leads relative to the centre of the MoS<sub>2</sub> central region, we calculated the transmission coefficient of the two structures shown below.

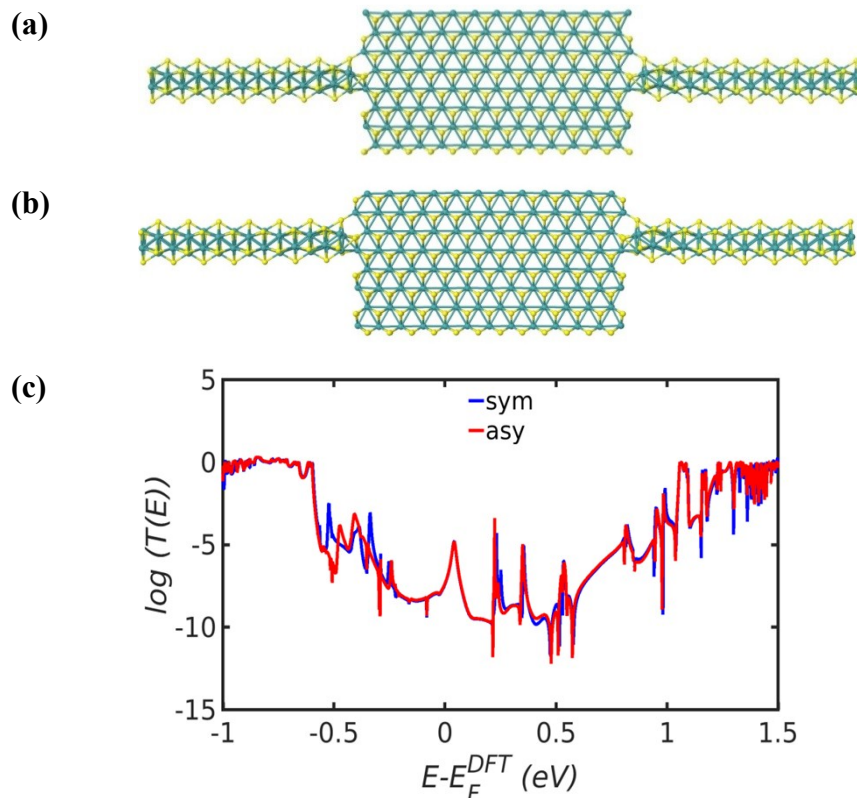


Fig. S5 (a) and (b) symmetric and asymmetric structures obtained by shifting the leads in the direction perpendicular to the transport direction; (c) transmission spectra of these two structures above. The blue represents the symmetric and the red is for the asymmetric structure.

## 6. Thermoelectric properties of configuration in S5(b)

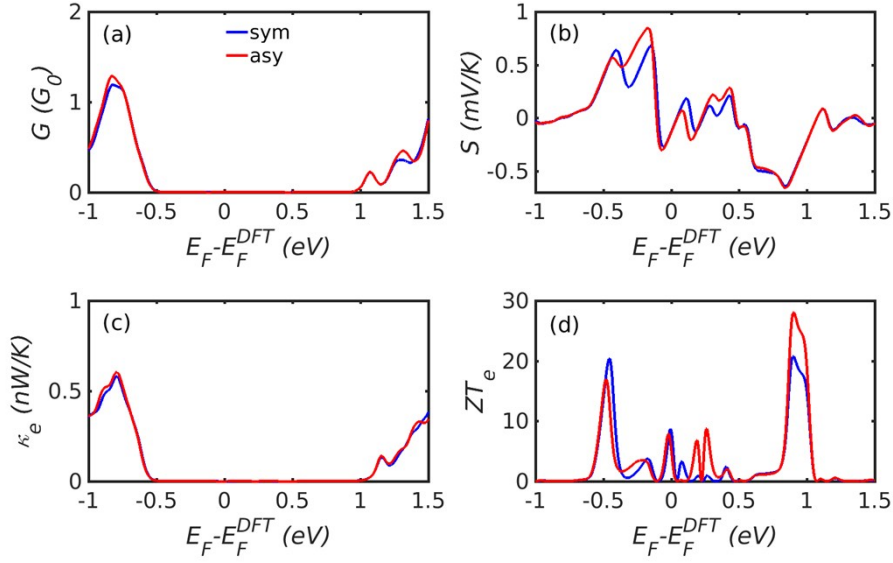


Fig. S6. Electronic contribution to room-temperature thermoelectric properties as a function of Fermi energy for the structure shown in Fig. S5(b). (a) Electrical conductance  $G$ , (b) Seebeck coefficient  $S$ , (c)-(d) electronic contribution to thermal conductance  $\kappa_e$  and to the thermoelectric figure of merit  $ZT_e$ .

## 7. Phonon transmission spectra for the configuration in Figure S5(b)

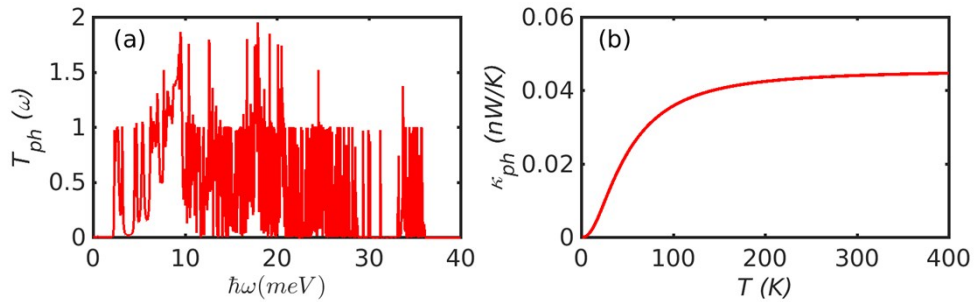


Fig. S7. (a) and (b) phonon transmission spectrum  $T_{ph}$  and thermal conductance  $\kappa_{ph}$  for the structure shown in Fig. S5(b).

## 8. Total ZT for configuration in S5(b)

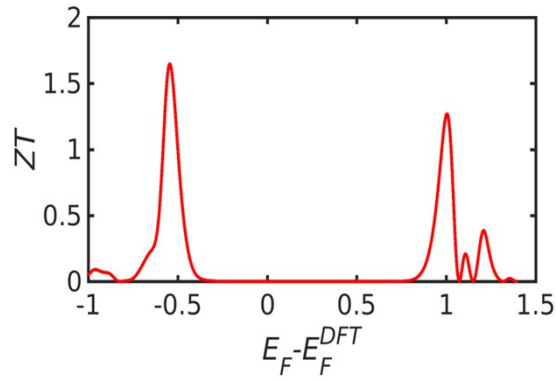
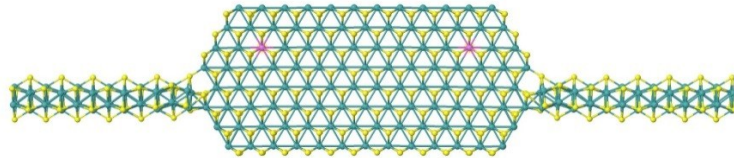


Fig. S8 Total thermoelectric figure of merit at 300 K for the structure shown in Fig. S5(b).

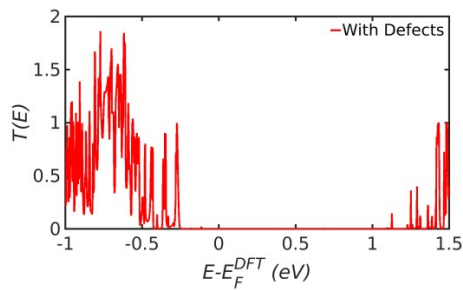
### 9. The results of replacing Mo with Nb substituents

To illustrate the effect of changing the positions and concentrations of dopant atoms, below we show transport properties obtained for the six different structures in boxes 1a to 6a. In each structure, the Nb dopant atoms are shown in red.

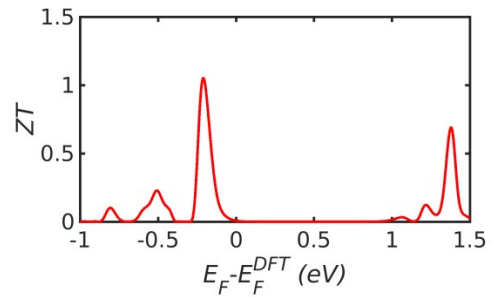
1(a)



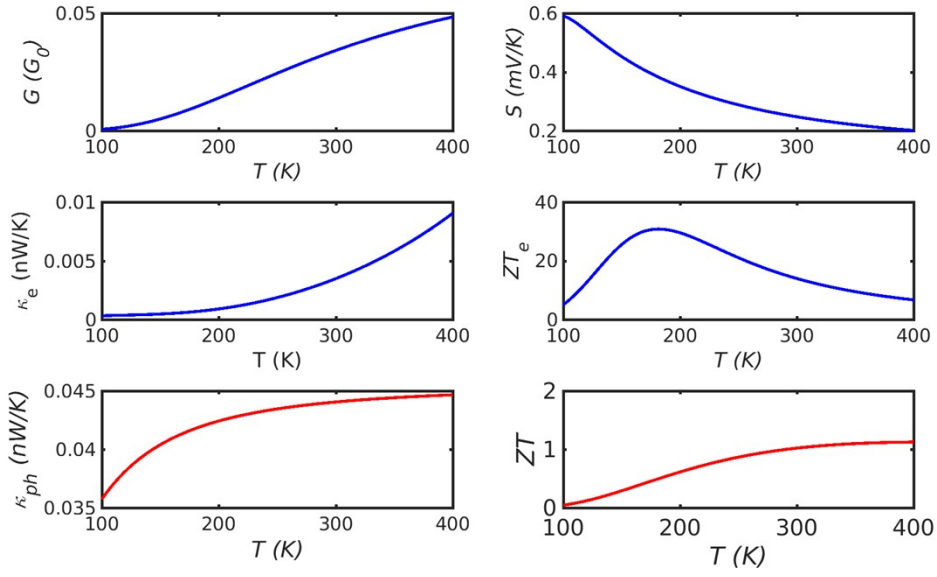
1(b)



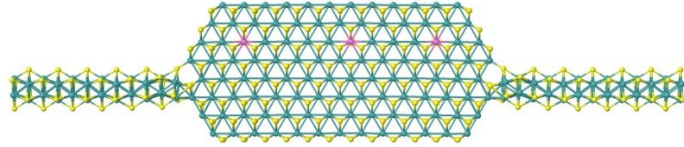
1(c)



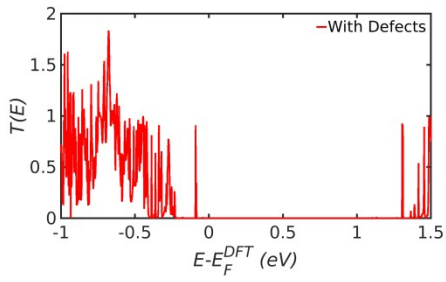
1(d)



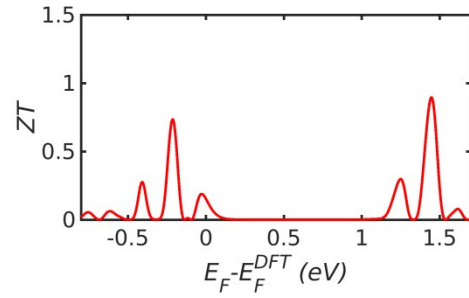
2(a)



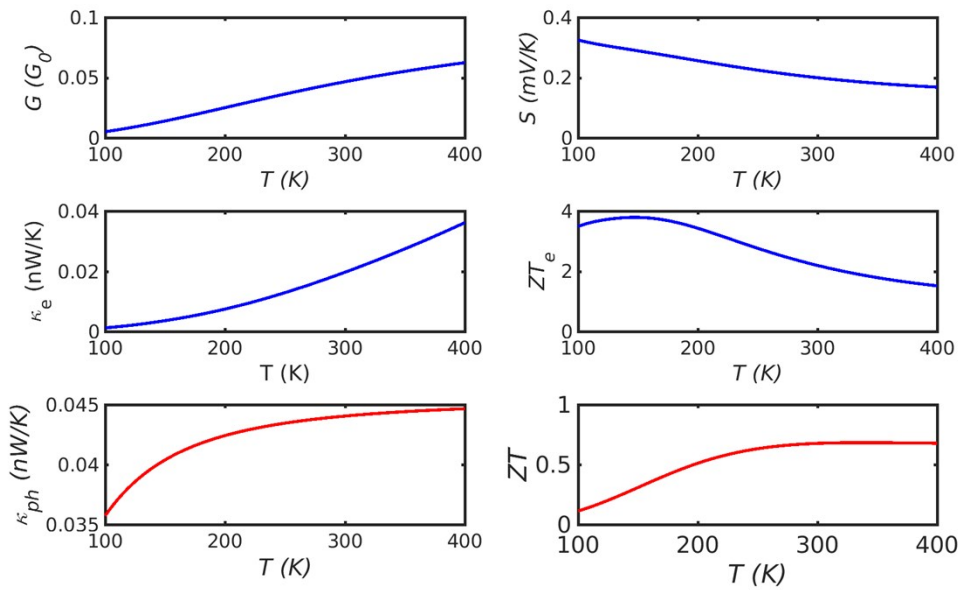
2(b)



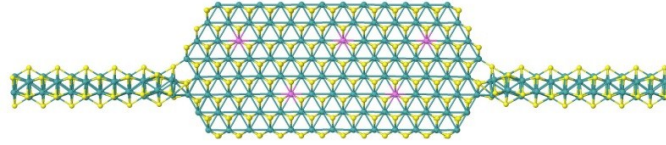
2(c)



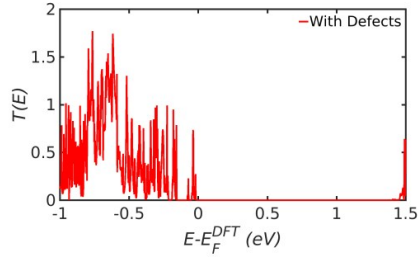
2(d)



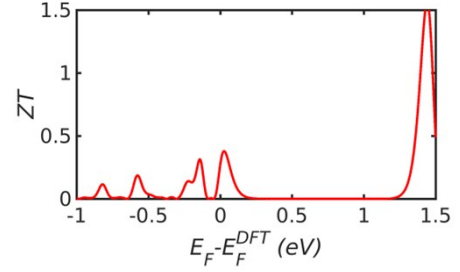
3(a)



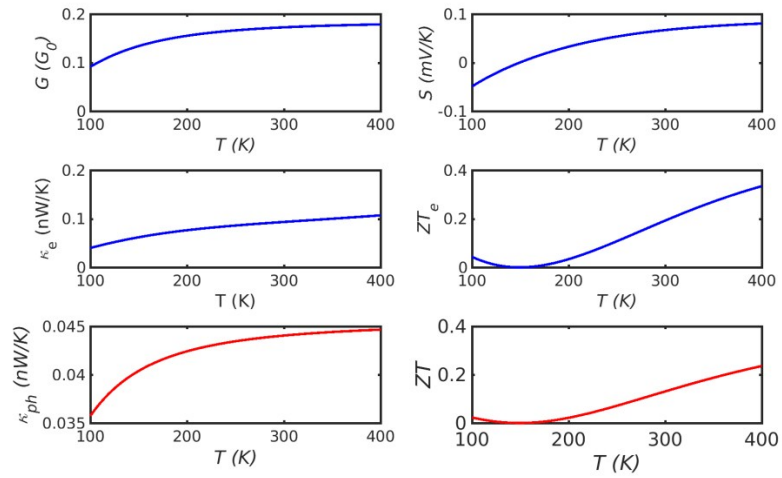
3(b)



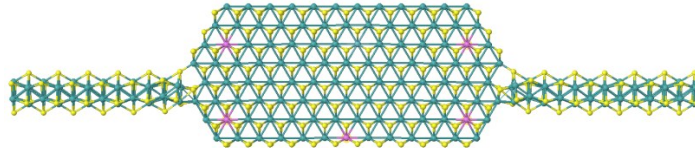
3(c)



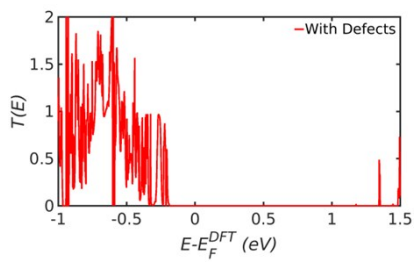
3(d)



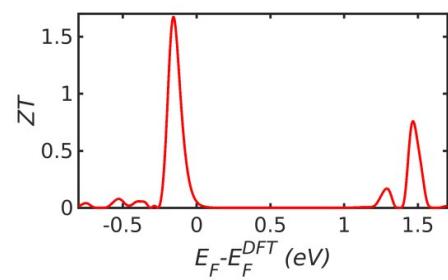
4(a)



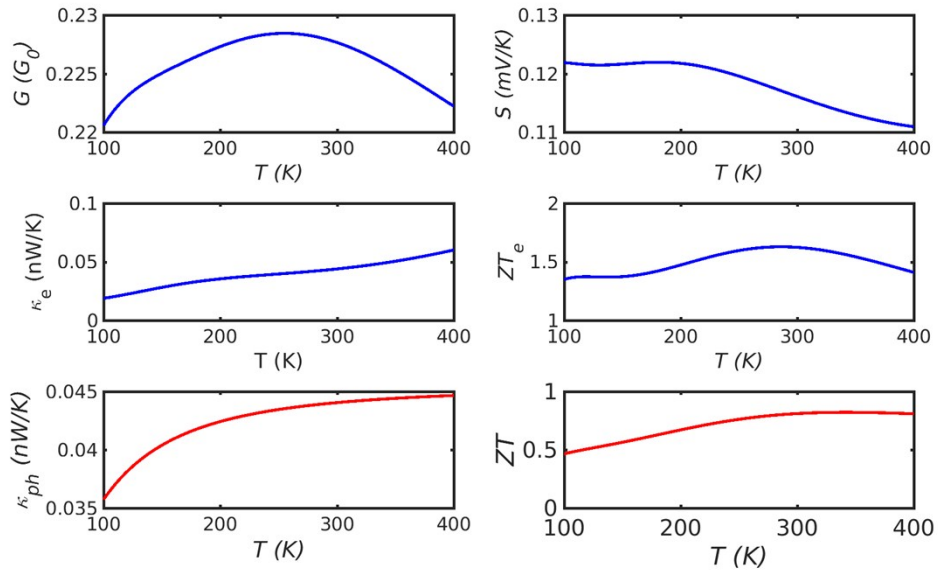
4(b)



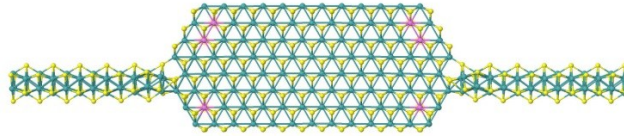
4(c)



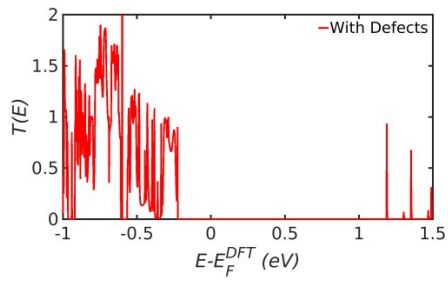
4(d)



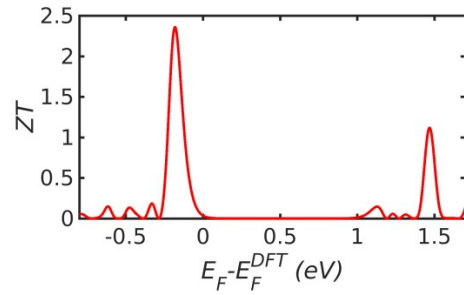
5(a)



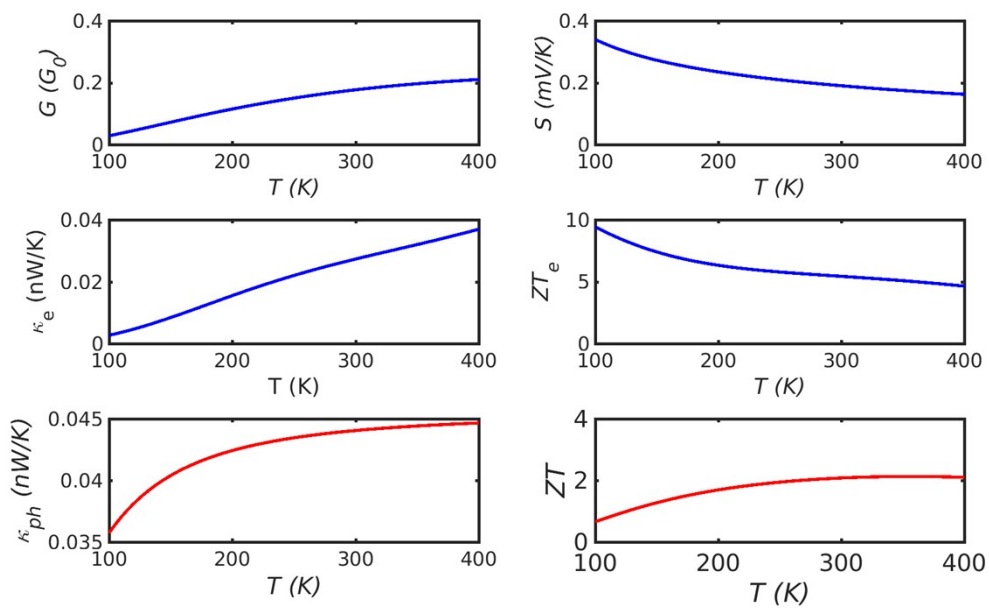
5(b)



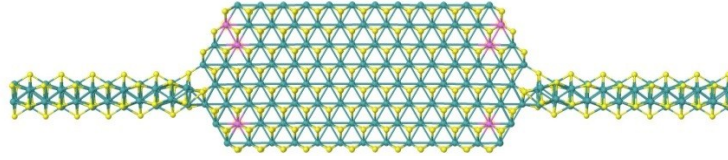
5(c)



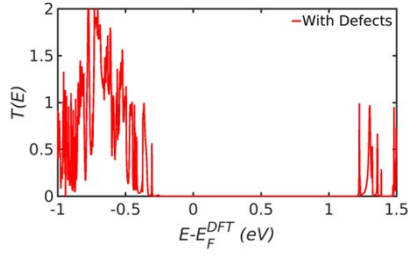
5(d)



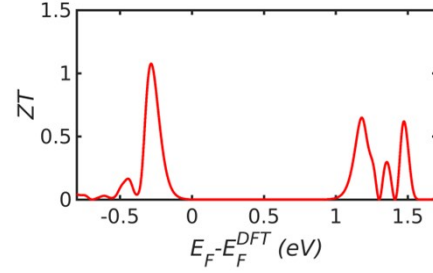
6(a)



6(b)



6(c)



6(d)

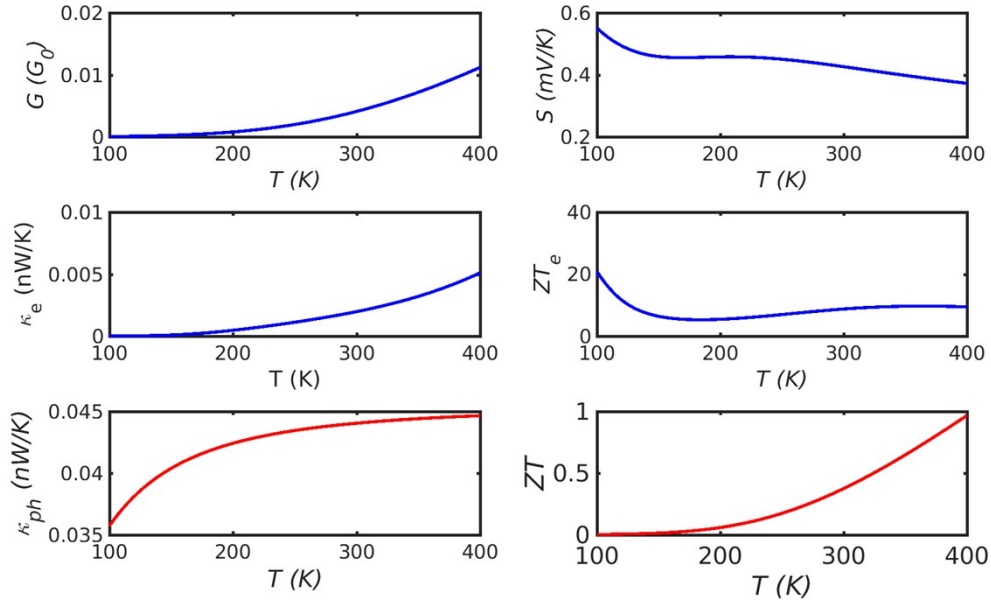


Fig. S9 (a) Configurations after doping Nb in the MoS<sub>2</sub> scattering region; (b) The corresponding transmission spectra; (c) The total thermoelectric figures of merit at 300 K. (d) The thermoelectric properties as a function of temperature when  $E_F - E_F^{DFT} = -0.2\text{eV}$ . The total ZT of all configurations increases with the temperature.

### 10. Formulae for ensemble averages of thermoelectric properties

Using the N=6 structures above, we compute ensemble-averaged quantities using the following formulae<sup>1</sup>:

$$S_{av} = \frac{\frac{1}{N} \sum_{i=1}^N G_i S_i}{\frac{1}{N} \sum_{i=1}^N G_i}$$

$$G_{av} = \frac{1}{N} \sum_{i=1}^N G_i$$

$$\kappa_{e_{av}} = \frac{1}{N} \sum_{i=1}^N \kappa_{ei}$$

$$ZT_{av} = \frac{S_{av}^2 G_{av} T}{\kappa_{e_{av}} + \kappa_{p_{av}}}$$

## 11. Relationship between the power efficiency and ZT.

ZT is a dimensionless measure of the efficiency, but not the efficiency itself. The maximum power efficiency  $\eta$  of a TE generator is a product of the Carnot efficiency  $\left(\frac{\Delta T}{T_h}\right)$  and a reduction factor

given by the material's figure of merit  $Z.T_{av} = \frac{S^2 G T_{av}}{\kappa}$  :

$$\eta = \frac{\Delta T}{T_h} \frac{\sqrt{[1 + Z.T_{av}] - 1}}{\sqrt{[1 + Z.T_{av}] + \frac{T_c}{T_h}}}$$

where  $T_h$  and  $T_c$  are the hot- and cold-side temperatures, respectively, and  $\Delta T = T_h - T_c$  and

$$T_{av} = \frac{T_h + T_c}{2}.$$

This shows that the largest power efficiency occurs when  $Z.T_{av}$  tends to infinity, ie when  $\kappa = 0$ .

## References

1. Quantum-Interference-Enhanced Thermoelectricity in Single Molecules and Molecular Films, Colin J. Lambert, Hatef. Sadeghi and Q. Al-Galiby, Comptes Rendus Physique, 17 (10) 1084 (2016)